

Short Communication

Electrochemical Properties of Single-crystalline Mn₃O₄ Nanostructures and their Capacitive Performance in Basic Electrolyte

Hidayat Ullah Shah¹, Fengping Wang^{1,*}, Arbab Mohammad Toufiq^{1,2,3}, Abdul Muqsit Khattak⁴, Azhar Iqbal⁴, Zahid Ali Ghazi⁴, Shujaat Ali¹, Xingyang Li¹, Ziya Wang¹

¹ Department of Physics, School of Mathematics and Physics, University of Science and Technology Beijing, Beijing 100083, P. R. China,

² Department of Physics, Hazara University Mansehra, Khyber Pakhtunkhwa, Mansehra, Pakistan

³ UNAM-National Nanotechnology Research Center, Institute of Materials Science and Nanotechnology, Bilkent University, Ankara 06800, Turkey

⁴ Laboratory for Nanomaterials, National Center for Nanoscience and Technology No. 11, Beiyitiaoyuan, Zhongguancun, Beijing 100190, PR China.

*E-mail: fpwang@ustb.edu.cn

Received: 13 June 2016 / Accepted: 15 July 2016 / Published: 6 September 2016

Single-crystalline Mn₃O₄ square-shaped nanostructures have been successfully synthesized by hydrothermal method without using any surfactant. The as-prepared products were characterized by X-ray diffraction (XRD), field emission scanning electron microscopy (FESEM), Transmission electron microscopy (TEM) and High Resolution transmission electron microscopy (HRTEM). To assess the potential properties of nanostructures, galvanostatic charging–discharging and cyclic voltammetry measurements were performed for their use in supercapacitors. The Mn₃O₄ nanoarchitectures used as supercapacitor electrode in 1 mol L⁻¹ KOH electrolyte have a specific capacitance value of 355.5 F g⁻¹ at a low current density of 0.35 A.g⁻¹. The device still retain 85.08% of its initial capacitance afterwards 2000 cycles at a current density of 5 A.g⁻¹. The as-synthesized Mn₃O₄ nanostructures exhibited a good rate capability and stability for electrochemical properties. These results indicate their potential application as electrode material for high performance supercapacitor in basic medium.

Keywords: Hydrothermal Method; Optical Properties; Transition metal oxides; Supercapacitance; Electrochemical properties;

1. INTRODUCTION

In recent few years, the esteemed demand of energy increased the importance of renewable energy resources and energy storage devices. Cost effective, high power performance, fast charge and

discharge rates, long cycle life and low maintenance catalyst has been a demanding challenge to solve the current energy crisis [1-2]. Researchers in both academic world and industry have deliberately increased efforts over the past decades to fabricate such an advanced materials with magnitudes ranging from a few to several hundred nanometers. The reason is that when particles are synthesis within a limit of around 1–100 nanometers, the materials' chemical and physical properties change considerably from those at bulk level. Nano-size materials are becoming increasingly significant for electrochemical energy storage [3].

Electrochemical capacitors (ECs), mostly referred by manufacturers in literature as “ultracapacitors,” or “supercapacitors” store energy using either fast surface redox reactions or ion adsorption. It can completely or less replace batteries in electrical energy storage appliances, where a high-power transfer is required. The ion desolvation approach in pores less than the solvated ions leads to higher capacitance for electrochemical double layer capacitors by means of carbon electrodes with nanometer pores, introduced new ways to construct high energy devices with different electrolytes. The discovery of carbon nanotubes brings revolution in electrochemical capacitors, permitting adaptable and innovative devices to be made [4-5].

Recently, different kinds of materials have been studied as possible supercapacitors electrodes, like, conducting polymers, carbonaceous materials, and transition metal oxides. Transition-metal oxides such as NiO [6], RuO₂ [7], Co₃O₄ [8] and MnO₂ [9] are mostly used electrode materials due to their large surface area, relatively better electrical conductivity and high capacitance. Among them, RuO₂ and MnO₂ are an ideal material for supercapacitors because of their variable oxidation states, good electrochemical and chemical stability, easy fabrication and high theoretical specific capacitance. However toxic nature, high cost and low porosity of RuO₂ restricts its commercialization in supercapacitors. Currently, MnO₂ is considered as one of the most promising candidate for supercapacitor application because of its abundant natural resources, non-toxicity, high capacitance and environmental friendliness. Manganese oxides have various forms such as MnO₂, MnO, Mn₂O₃ and Mn₃O₄, due to its different oxidation states. Among these manganese oxides, Mn₃O₄ is one of the established mixed oxides state (Mn²⁺(Mn³⁺)₂O₄) with spinel structure. Mn₃O₄ has been broadly used in different fields such as electrode material for supercapacitor and lithium batteries [10-13], an effective catalyst for the decay of waste gaseous products and an appropriate material to control the air pollution [12].

It should be noted that the capacitance of the capacitor depends mostly on the capacity of electrode material expressed in farad/gram (F.g⁻¹), while the voltage and the resistance of such device depends mainly on the electrolyte. Lota *et al.* tried to find the inert electrolyte, such as Na₂SO₄, Na₂SO₃, K₂SO₄, Li₂SO₄, (as well as for comparison 1 M H₂SO₄ and 6 M KOH) and evaluate their effect on the capacitance of electrode materials (two activated carbons and carbon nanotubes) to the electrochemical capacitor. The highest values of conductivity were obtained for 1 M H₂SO₄ and 6 M KOH, while MgSO₄ has the lowest conductivity from electrolytes which were selected. [13].

In our previous work, we have reported 3D nanostructures, self-assembled with single-crystalline Mn₃O₄ nanoparticles and their multiple PL emissions in visible region without any surface modification [14]. Wu *et al.* have studied the electrochemical performances of porous calcium carbide-derived carbon (CCDC) material for supercapacitors in different aqueous electrolytes such as KOH,

K_2SO_4 , KCl and KNO_3 . Among all the tested electrolytes, KOH solution has shown the highest specific capacitance that is endorsed to the fast mobility of OH^- ions [15]. To the best of our knowledge, very less literature is available about Mn_3O_4 material been checked in basic medium. In this study, we synthesis pure Mn_3O_4 nanostructure by hydrothermal method and estimated the electrochemical performances in 1 M KOH solution. The supercapacitor exhibited excellent cycling performance as the device retain 85.08% of its initial capacitance after 2000 cycles at a current density of $5 A.g^{-1}$.

2. EXPERIMENTAL DETAILS

2.1. Sample preparation

The chemical reagents used in this research work were of analytical grade and used without any additional refinement. In a typical reaction, 1.5g of manganese Chloride Tetrahydrate ($MnCl_2.4H_2O$) was dissolved in 40ml deionized water through magnetic stirring for 20 minutes at room temperature. After that, 1.6 g of NaOH was mixed to the solution and stirred further for 20 minutes. Finally, the homogeneous solution was transferred into a 40 mL Teflon-lined stainless steel autoclave and hydrothermally reacted at $180C^0$ for 18 h in an oven. The reaction suspension was centrifuged, filtered and washed several times with H_2O and ethanol to remove the residual traces. The brown precipitate were dried at $90C^0$ for 6 h.

2.2. Sample Characterizations

The crystallographic and phase study of the as-prepared product were investigated by X-ray diffractometer (X'Pert MPD-XRD) having Cu $K\alpha$ radiation ($\lambda= 0.154nm$, 40 KV, 40mA), field emission scanning electron microscopy (FESEM, ZEISS SUPPERTM 55) and high resolution transmission electron microscopy (HRTEM) and selected area electron diffraction (SAED JEM 2010). The electrochemical properties were measured with 1M KOH as the electrolyte in a three-electrode configuration. The electrode (working) was prepared by mixing 70 wt.% Mn_3O_4 powder as an active materials, 25 wt.% acetylene black, as the conductive filler and 5 wt.% polyvinylidene fluoride (PVDF), as the binder. Proper quantity of water was added to this mixture to make homogenous slurry, further pasted on Ni-foam which acts as working electrode and as current collector. The cyclic voltammetry (CV) and galvanostatic charge–discharge tests were conducted with CHI 660C electrochemical workstation.

3. RESULTS AND DISCUSSION

3.1. XRD analysis

The XRD pattern of Mn_3O_4 is depicted in fig. 1. All the diffraction peaks are well indexed to the Hausmannite (Mn_3O_4) tetragonal crystal structure (JCPDS file No. 80-0382) [16-17]. No other characteristic peaks from impurities are found, demonstrating the high purity of the as-prepared product. The sharp diffraction peaks of the XRD patterns specify that the as-prepared products are well

crystallized. The EDX analysis illustrated in the upper inset of Fig. 1, shows that the final brown precipitate comprises only Mn and O which shows that the as-synthesized products are made of pure Mn₃O₄.

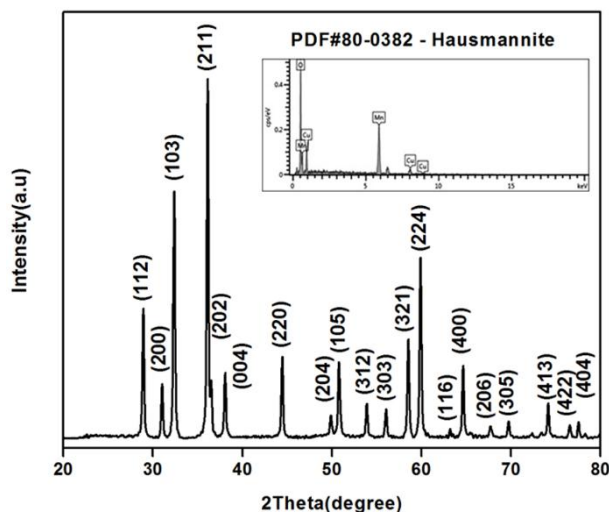


Figure 1. XRD pattern of as-prepared Mn₃O₄ nanostructures

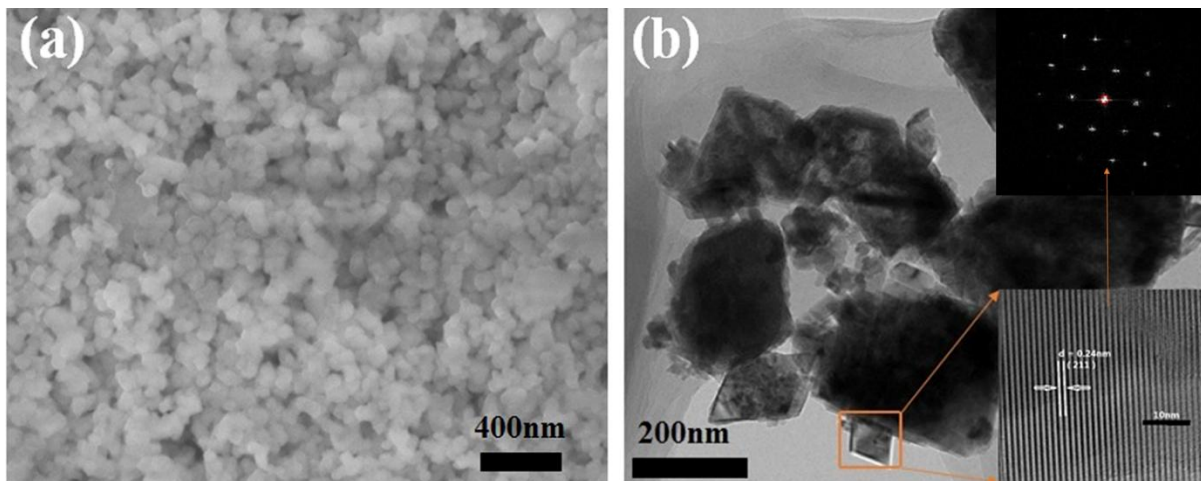


Figure 2. (a) FESEM (b) TEM and HRTEM images of as-prepared Mn₃O₄ nanostructure

The morphology of the Mn₃O₄ nanostructures was primarily imaged by FESEM as shown in Fig 2 (a). The FESEM image shown in Fig. 2a demonstrates that as-prepared Mn₃O₄ consists of squared-shape, identical, and uniform nanoparticles with diameter of about 70nm. More detailed information regarding the structural aspects of the Mn₃O₄ nano-structures has been investigated by TEM and HRTEM. Fig. 2b illustrates the TEM image of Mn₃O₄ nanostructures, which is in agreement with FESEM observations. The HRTEM image taken from a randomly distributed nanoparticle given in lower inset of fig.2 (b) demonstrated the singlet set of parallel planes with inter-planer (*d*) spacing of 0.24nm, which correspond to the *d* spacing of [211] plane of Mn₃O₄ in the XRD spectrum. The single

crystalline structure of as-prepared Mn_3O_4 nanostructures is also verified by the SAED pattern presented in the upper inset of fig.2 (b).

3.2. Electrochemical Characterization

Electrochemical properties of Mn_3O_4 electrode were examined by cyclic voltammetry (CV) and galvanostatic charge–discharge tests in 1 M aqueous KOH electrolyte. The specific capacitance can be determined by integrating the area under the curve (CV) to obtain the charge (Q) and then dividing by the mass of the electro active material (m), the scan rate (v), and the potential window ($\Delta V = V_a - V_c$) according to the equation 1.

$$C = \frac{Q}{\Delta V} = \frac{1}{mv(V_a - V_c)} \int_{V_a}^{V_c} I(V) dV$$

Furthermore, the specific capacitance was computed from the galvanostatic charging–discharging curves using equation 2.

$$C = \frac{I \Delta t}{\Delta V m}$$

Where C stands for specific capacitance, I is the current density, Δt for discharge time, ΔV is the potential window and m is the active mass of material [18].

Fig. 3(a,b) shows the Cyclic voltammetric (CV) analysis carried out in the voltage range of -0.25 to 0.45 V vs. Ag/AgCl in 1 M KOH solution. Fig. 3(a) shows the CV curves of Mn_3O_4 electrode at different scan rates of 10, 20, 50, 80, 100 and 200 mV s^{-1} , respectively. The cathodic and anodic peaks observed in the cyclic voltammograms point towards the reversible oxidation and reduction reaction. More specifically, a pair of redox reaction peaks in the CV curves of the synthesized Mn_3O_4 nanoparticles clearly suggesting the pseudo-capacitance behavior that can be attributed to the redox transitions of interfacial oxidation species at various Mn oxidation states (i.e., Mn^{2+} and Mn^{3+}). The pseudo-capacitance mechanism of Mn_3O_4 electrode can be explained using following relations [19];



In Fig.3a, it can be seen that even at high sweep rate of 200 mV s^{-1} , the CV curve of Mn_3O_4 electrode retains its shape which reveals the enhanced electrochemical reversibility of the faradic redox reaction of Mn_3O_4 electrode. Furthermore, an ideal capacitive behavior is evident by the increase in redox current with respect to the scan rate which also verify the good rate capability of our synthesized material [20]. It can be observed that the redox peaks undergoes negative and positive shifts by increasing the scan rate, which can be attributed to the resistance of the electrode [18]. The electrochemical stability of the as-synthesized Mn_3O_4 electrode material was investigated by repeating the CV test measured at a scan rate of 80 mVs^{-1} for 500 cycles shown in Fig 3b. The CV curves shows no significant variation after 500 cycles which indicates the excellent cycling stability of the Mn_3O_4 electrode. The CV investigations reveal stable electrochemical performance and suggests that as-prepared Mn_3O_4 electrode has potential application due to the enhanced capacitive behavior.

Galvanostatic charge/discharge curves of Mn_3O_4 electrode for the first 10 cycles at constant current density of 10 A.g^{-1} are plotted in figure 3(d). The charge/discharge curves shows the pseudo-capacitance nature of the Mn_3O_4 electrode. Figure 6(c) shows the discharge curves of Mn_3O_4 electrode

at different current densities (i.e., 0.35, 0.5, 0.8, 1, 2.5, 5 and 10 A.g⁻¹). These curves show that at higher current density the specific capacitance values decreases due to the intercalation of ions at the surface of the active materials in the electrode/ electrolyte interface whereas at low current density the specific capacitance increases due to the intercalation/ de-intercalation of ions at surface and inner matrix of the active materials.

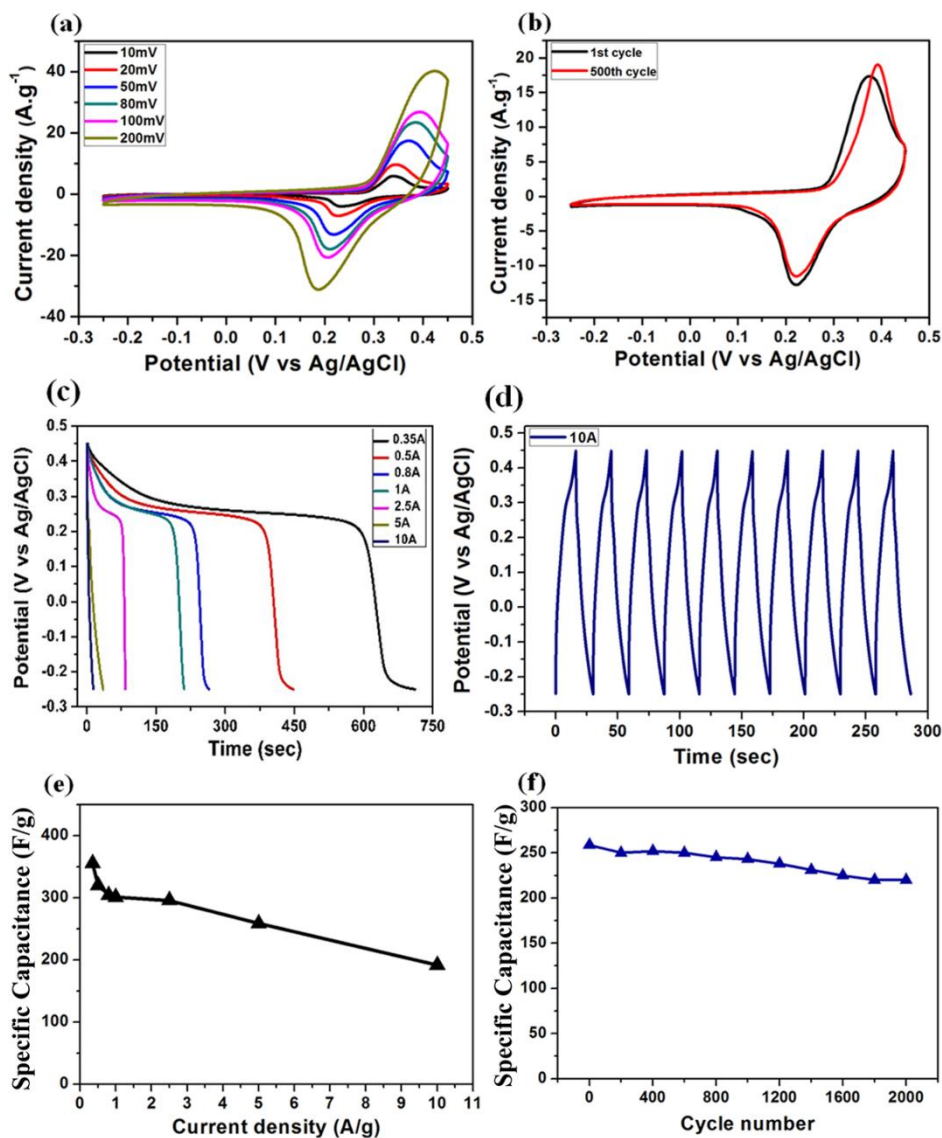


Figure 3. CV and charging-discharging curves, corresponding specific capacitance, and capacitance retention of Mn₃O₄ electrode. (a) CV curves of Mn₃O₄ electrode at different potential scan rates from 10 to 200 mV s⁻¹; (b) Cycling stability of Mn₃O₄ electrode at 80 mV/s ; (c)charge–discharge curves of Mn₃O₄ electrode at different current densities from 0.35 to 10 A.g⁻¹; (d) First 10 Galvanostatic charge-discharge curves of Mn₃O₄ electrode at the current density of 10 A.g⁻¹; (e) the corresponding specific capacitance as a function of current density; (f) Capacitance retention of the Mn₃O₄ electrode at 5 A.g⁻¹ as a function of cycle number.

The specific capacitances of the synthesized Mn_3O_4 electrode material as a function of different current densities are shown in Fig. 3(e), which are in agreement to the results obtained from the discharge curves plotted in Fig. 3d.

The electrochemical stability is a key property of an electrode material for potential applications of supercapacitors at high current density. Therefore, the cyclic stability test has been accomplished at high current density of 5 A g^{-1} in the potential range of -0.25 to $0.45 \text{ V vs. Ag/AgCl}$ in 1 M KOH solution. The stability curve plotted in Fig. 3(f), evident that the as-prepared Mn_3O_4 electrode demonstrates excellent stability over 2000 cycles with negligible capacitance degradation. The value of capacitance measured at first cycle is calculated to be 258.57 F g^{-1} which reduced to 220 F g^{-1} after 2000 cycles that corresponds to a capacitance loss of 85.08% . These results indicate that the as-synthesized Mn_3O_4 nanostructure is highly stable in the long term repeated charge/ discharge cycles as supercapacitors electrode material. We believe, that the enhanced stability at high current density values may be attributed to the uniform particle morphology which enables the electron transport from the electrode/electrolyte interface and low resistance of the electrode material. These structural and electrochemical results strongly suggests that the as-prepared Mn_3O_4 nanomaterial has potential applications to be used as supercapacitors.

The calculated capacitance value 355.5 F g^{-1} is much higher than the reported values for Mn_3O_4 . Yuqing Qiao *et al.* reported a specific capacitance of 286 F.g^{-1} (in $1 \text{ mol L}^{-1} \text{ Na}_2\text{SO}_4$ electrolyte at a low current density of 0.5 A.g^{-1}) for micro/nano-structured Mn_3O_4 fabricated by a facile solvothermal approach [21]. A specific capacitance of 263 F.g^{-1} (in 4 M NaOH electrolyte at a current density of 1 A.g^{-1}) for Mn_3O_4 nanorods grown on Ni foam synthesized by hydrothermal method have also been reported [22], Guo-rong *et al.* reported a specific capacitance of 230 F.g^{-1} (in $0.5 \text{ mol L}^{-1} \text{ Na}_2\text{SO}_4$ electrolyte at a current rate of 0.25 A.g^{-1}) for Ni- Mn_3O_4 nanocomposite prepared by chemical method [23].

4. CONCLUSION

In summary, we reported the evolution of single crystalline square-shaped Mn_3O_4 nanostructures with uniform using hydrothermal-growth method. The as-prepared material can improve not only the initial discharge capacity, but also the cycling stability during subsequent cycles. Furthermore, this research effort can give rise to an enhanced performance in the case of graphene/ Mn_3O_4 composite. A high specific capacitance of 355.5 F g^{-1} at 0.35 A.g^{-1} measured for the as-synthesized Mn_3O_4 nanostructures makes this material interesting for potential applications in supercapacitors electrode material and rechargeable lithium-ion batteries.

ACKNOWLEDGEMENTS

We appreciate the financial supports of the National Key Scientific Instruments and Equipment Development Special Fund (2011YQ14014506 and 2011YQ14014507), China (2012), University of Science and technology Beijing (fundamental development and Chinese Government Scholarship

program) and the fundamental Research Funds for the Central Universities: Chinese government scholarship program.

References

- 1 G. Han, Y. Liu, L. Zhang, E. Kan, S. Zhang, J. Tang and W. Tang, *Sci. Rep.*, 4 (2014) 4824.
- 2 L. Wang, Y. Li, Z. Han, L. Chen, B. Qian, X. Jiang, J. Pinto and G. Yang, *J. Mater. Chem. A*, 1 (2013) 8385–8397.
- 3 A. S. Aricò, P. Bruce, B. Scrosati, J.-M. Tarascon and W. van Schalkwijk, *Nat. Mater.*, 4 (2005) 366–377.
- 4 P. Simon and Y. Gogotsi, *Nat. Mater.*, 7 (2008) 845–854.
- 5 An, Kay Hyeok, Won Seok Kim, Young Soo Park, Young Chul Choi, Seung Mi Lee, Dong Chul Chung, Dong Jae Bae, Seong Chu Lim and YHL *Adv. Mater.*, 13 (2001) 497–500.
- 6 S. Vijayakumar, S. Nagamuthu and G. Muralidharan, *ACS Appl. Mater. Interfaces.*, 5 (2013) 2188–2196.
- 7 T. Liu, W. G. Pell and B. E. Conway, *Electrochim. Acta.*, 42 (1997) 3541–3552.
- 8 A. Xiao, S. Zhou, C. Zuo, Y. Zhuan and X. Ding, *Mater. Res. Bull.*, 60 (2014) 674–678.
- 9 N. Metals, *Transactions Nonferrous Met. Soc. China*, 17 (2007) 5–9.
- 10 T. Wang, Z. Peng, Y. Wang, J. Tang and G. Zheng, *Sci. Rep.*, 3 (2013) 2693.
- 11 H. Tang, Y. Sui, X. Zhu and Z. Bao, *Nanoscale Res. Lett.*, 10 (2015) 260.
- 12 G. Laugel, J. Arichi, H. Guerba, M. Molière, a. Kiennemann, F. Garin and B. Louis, *Catal. Letters.*, 125 (2008) 14–21.
- 13 K. Lota, A. Sierczynska and I. Acznik. *CHEMIK.*, 67 (2013) 1142–1145.
- 14 A. M. Toufiq, F. Wang, Q.-U.-A. Javed, Q. Li, Y. Li and M. Khan, *Mater. Express.*, 4 (2014) 258–262.
- 15 H. Wu, X. Wang, L. Jiang, C. Wu, Q. Zhao, X. Liu, B. Hu and L. Yi, *J. Power Sources*, 226 (2013) 202–209.
- 16 V. C. Bose, K. Maniammal, G. Madhu, C. L. Veenas, A. S. A. Raj and V. Biju, *IOP Conf. Ser. Mater. Sci. Eng.*, 73 (2015) 012084.
- 17 MIMIC. Hen, XIZ. Hou, CSU. Hangwei, MIX. Iang and JUGUo, *Asian Journal of Chemistry*; 26 (2014) 714–718.
- 18 Y. G. Wang, H. Q. Li and Y. Y. Xia, *Adv. Mater.*, 18 (2006) 2619–2623.
- 19 L. He, G. Zhang, Y. Dong, Z. Zhang, S. Xue and X. Jiang, *Nano-Micro Lett.*, 6 (2014) 38–45.
- 20 S. Nagamuthu, S. Vijayakumar and G. Muralidharan, *Energy and Fuels.*, 27 (2013) 3508–3515.
- 21 Y. Qiao, Q. Sun, H. Cui, D. Wang, F. Yang and X. Wang, *RSC Adv.*, 5 (2015) 31942–31946.
- 22 D. Li, F. Meng, X. Yan, L. Yang, H. Heng and Y. Zhu. *Nanoscale Res Lett.*, 19 (2013) 535.
- 23 G. Xu, J. Shi, W. Dong, Y. Wen, X. Min and A. Tang, *J. Alloys Compd.*, 630 (2015) 266–271.